JOURNAL OF MATERIALS SCIENCE 37 (2002) 1347–1354

Effect of aluminium silicate filler on morphology and physical properties of closed cell microcellular ethylene–octene copolymer

N. C. NAYAK, D. K. TRIPATHY*
Rubber Technology Centre, Indian Institute of Technology, Kharagpur 721302, India
E-mail: dkt@rtc.iitkgp.ernet.in

The effect of aluminium silicate filler on the morphology of the microcellular ethylene–octene copolymer (Engage) has been studied from SEM photomicrographs with variation of blowing agent and silicate filler loading in comparison to the unfilled vulcanizates. The average cell size, maximum cell size and cell density varies with variation of blowing agent and filler loading. Physical properties like relative density, hardness, tensile strength, elongation at break, modulus, tear strength decreases with blowing agent concentration. However tensile strength, modulus (100%), tear energy and hardness varies linearly with the density of the filled vulcanizates. The elastic nature of closed cells reduces the hysteresis loss compared to solid compounds. Set properties improve with blowing agent concentration. It is observed that stress relaxation behavior is independent of blowing agent loading i,e., density of closed cell microcellular vulcanizates. Theoretically flaw sizes are found to be about 2.57 times larger than maximum cell sizes observed from SEM photomicrographs.

1. Introduction

Crosslinked polyolefin foams posses tremendous potential due to their wide variety of properties such as light weight, buoyancy, chemical resistance, inertness, good aging, cushioning performance, thermal and acoustic insulation and recyclability but they do not provide a high enough state of physical properties at a given flexibility to fully compete with the cellular elastomer market. Polyolefin resin made with conventional catalyst technology exhibit relatively wide molecular weight distribution and non-uniform branch structure. This non-uniformity contributes to the inability of polyolefins to provide the high state of physical properties offered by cellular elastomer [1, 2].

The development of Dow's INSITE^{TM} constrained geometry catalyst technology (CGCT) has led to the polymerization of ultra-low-density ethylene-octene copolymers as well as copolymers with densities in the range of conventional LLDPEs. Copolymers with densities less than 0.90 g/cc synthesized with this technology constitute a unique class of thermoplastic elastomers [3]. The grades those are of particular interest to rubber industry, are the grades with high comonomer content because this gives highly amorphous products with very low density. Materials with density lower than about 0.885 have been designated as "polyolefin elastomers" (POE) [4]. In 1993, Dow Pont Dow Elastomer has introduced POEs under the brand name ENGAGE. They are ethylene-octene copolymers produced via advanced INSITE^{TM} catalyst and process technology designed to be processed like thermoplastic but can be compounded like elastomers. The exceptional performance of Engage is attributed to extraordinary control over polymer structure, molecular weight distribution, uniform comonomer composition and rheology. They are being considered for use in divers applications such as cushioning agents, gaskets, and particularly good alternative for sealing application due to their structural regularity and non-toxic composition. Foam made from these metallocene-based polyolefins (MPO) have been recently commercialized and are being considered for use in diverse applications as cushioning agents, gaskets, sealants, etc. [5]. However industrial and commercial applications of microcellular elastomers demand strong, smooth skin and uniform cell structure. Close control of foam structure depends on the proper selection of blowing agents and curatives to achieve the correct balance between gas generation and degree of cure. The morphology of elastomeric foam [6] and characterization of microcellular foam [7] have also been reported. Mechanical properties and modeling of cellular materials of polymers, ceramics and metals have been published by several authors [8–10]. Theoretical modeling of elastomeric latex foam has been developed by some researchers for both open and closed cell foam to predict the failure properties [11–14]. The mechanism of nucleation and bubble growth in elastomers [15], thermoplastics [16], thermoplastic elastomer [17] and microcellular thermoplastics [18–20] using blowing agent and super saturated methods have

*Author to whom all correspondence should be addressed.

been the subject of recent research. Recently morphological, physico-mechanical properties of cellular and microcellular rubbers such as hysteresis, damping, cell size and thermal insulation properties have been reported [21–27]. This paper reports the morphology and physico-mechanical properties of closed cell microcellular ethylene-octene copolymer with special reference to the effect of blowing agent and aluminium silicate filler loading.

2. Experimental

2.1. Materials

Engage-8150 (ethylene-octene copolymer) containing 25% wt octene monomer with a melt flow index 0.5 g/10 min (190°C/2.16 kg), density 0.868 gm/cc, Mooney viscosity, ML_{1+4} (121°C) 35, manufactured by Du Pont Dow Elastomer Co has been used. The filler used was aluminium silicate, manufactured by Bagri Minerals and Chemicals Limited, India, having specific gravity 2.5; BET surface area, 16–17 m^2/g; oil absorption as per IS: 505 is 60 ± 5 and mean particle size (D 50) is 1–1.5 μm. The dicumyl peroxide (DCP) used was of 98% purity, manufactured by Aldrich Chemical Company, USA. Azodicarbonamide (ADC), the blowing agent used was of ADC-21, manufactured by High Polymer Lab, India.

2.2. Compounding and sample preparation

Engage was compounded with the ingredients according to the formulations of the mixes (Table I). Compounding was done in a Brabender Plasticoder (model, PLE 330) having cam type rotors. The engage was first melted at 80°C with rotor speed of 60 rpm for two minutes followed by addition of other ingredients. With subsequent incorporation of filler mixing was continued for another three minutes to ensure homogeneous distribution of ingredients. In case of filled compounds blowing agent was added along with the filler for good dispersion. Finally curative was added. The hot mix was taken out and passed through tight nip two-roll mill to form a sheet. Cure characteristics of the vulcanizates were determined in a Monsanto Rheometer, R-100. The vulcanizates were moulded at 160°C to 80% of their respective optimum cure times in an electrically heated hydraulic press at a pressure of 5 MPa. All the sides of the mould were tapered to 30° to facilitate the expansion of the microcellular product and for better mould release. Expanded microcellular sheets were post cured at 100°C for one hour in an electrically heated air oven.

2.3. Test procedures

Densities of the samples were determined according to ASTM D 3574-86. Hardness was measured using Shore A Durometer as per ASTM D 676-59 T. Stress–strain properties such as tensile strength, elongation at break, modulus and hysteresis were determined on a Zwick Universial Testing machine at room temperature (25 ± 2°C) according to ASTM D 3574-86. Cresent tear strength and trouser tear strength were also measured in the Zwick as per ASTM D 3574-86. Stress relaxation was measured according to ASTM D 3574. Mooney Viscosity was determined according to ASTM D1446-1963 by using Negretti Automatic Shearing Viscometer, model MK-III, UK. At least three samples were tested for each property and the mean values were reported.

SEM Studies were carried out for determination of cell structure using JEOL JSM 5800 Scanning Electron Microscope. Razor-cut surfaces from microcellular sheets as well as fractured surfaces of the tensile specimen were used as samples for SEM studies. The samples were gold coated before being studied.

3. Results and discussion

3.1. Rheometric characteristics

The cure characteristics of the vulcanizates containing blowing agent and aluminium silicate filler, obtained from Monsanto rheographs are summarized in Table II. It is seen that in both unfilled and aluminium silicate filled systems maximum rheometric torque

TABLE II Rheometric characteristics of unfilled and alumunium silicate filled vulcanizates

Mix no	Mooney viscosity (ML_{1+4} 100°C)	Minimum rheometric torque (dN · m)	Maximum rheometric torque (dN · m)	Rheometric scorch time at 160°C (min)	Optimum cure time at 160°C (min)
G_0	48	8.5	46	1.25	18
G_2	48	8	38	1.25	18.5
G_4	47	8	28	1.5	19
G_6	46	8	19	1.5	21
EAS_1	55	14.5	47	1.25	20
EAS_2	54	14	44	1.25	24.5
EAS_3	53	13.5	30	1.5	25
EAS_4	52	13	25	1.5	28
EAS_5	57	15.5	46	1.25	24
EAS_6	56	15	41	1.25	25
EAS_7	55	14.5	26.5	1.5	26
EAS_8	53	14	25.5	1.5	30

TABLE I Formulations of unfilled and aluminium silicate filled vulcanizates

	Mix no.											
	G_0	G_2	G_4	G_6	EAS_1	EAS_2	EAS_3	EAS_4	EAS_5	EAS_6	EAS_7	EAS_8
Engage	100	100	100	100	100	100	100	100	100	100	100	100
Aluminium Silicate	0	0	0	0	30	30	30	30	45	45	45	45
Parrafin Oil	2	2	2	2	4	4	4	4	6	6	6	6
ADC-21	0	2	4	6	0	2	4	6	0	2	4	6
DEG	–	–	–	–	2	2	2	2	3	3	3	3

Each mix contains ZnO, 3; Stearic Acid, 1; and Dicumyl peroxide(DCP 98%), 1.2 p hr.

decreases with increase in blowing agent concentration. This decrease in maximum torque is due to decomposition of blowing agent and the decomposed gas form microbubbles. These microbubbles reduce the melt viscosity and hence maximum torque decreases. With incorporation of filler, minimum rheometric torque increases but the maximum rheometric torque decrease marginally. However there is significant change in Mooney Viscosity values. Rheometric scorch time (t_2) increases marginally with increasing blowing agent concentration and filler loading. The optimum cure time increases with increase in blowing agent and filler concentration. Curing is effected by the exothermic decomposition of blowing agent. Therefor the actual cure characteristics can not be obtained from the rheographs whereas the resultant effect of curing and blowing can be obtained.

3.2. Morphology of razor-cut surfaces

The SEM photomicrographs of various unfilled and aluminium silicate filled microcellular vulcanizates are shown in Fig. 1. These photomicrograpgs are analysed in terms of average cell size or diameter, maximum cell size and cell density (no of cells per unit volume). The results are summarized in Table III. It is seen that the average cell size decreases with increasing blowing agent loading as well with the increase in aluminium silicate filler loading. However maximum cell size increases with increasing filler loading. It is observed that addition of filler increases the number of cells and also

TABLE III Physical properties of unfilled and aluminium silicate filled vulcanizates

Mixes	Relative density	Hardness (shore A)	Average cell size (μm)	Maximum cell size (μm)	Cell density $N = 6/\pi d^3$ $[\rho_s/\rho_f - 1]$ m^{-3}
G_2	0.722	50	27	60	3.72×10^{13}
G_4	0.577	32	26	60	7.9×10^{13}
G_6	0.477	22	23	55	1.71×10^{14}
EAS_2	0.66	53	27	64	5.26×10^{13}
EAS_3	0.414	39	26	60	1.58×10^{14}
EAS_4	0.328	31	25	56	3.93×10^{14}
EAS_6	0.589	50	26	73	1.49×10^{14}
EAS_7	0.374	32	25	56	3.65×10^{14}
EAS_8	0.302	28	24	54	6.31×10^{14}

reduces the average cell size. Increase in number of cells may be considered to be due to the nucleation by filler surfaces and decrease in cell size is attributed to the increase in melt viscosity by incorporation of silicate filler which retards the growth of cells. The number of cells per unit volume (m^{-3}) of the microcellular vulcanizates at maximum expansion is calculated by using the following relation [6]:

$$N = 6/\pi d^3[\rho_s/\rho_m - 1] \quad (1)$$

where N is the number of cells per unit volume; d, the average cell diameter; and ρ_s and ρ_m, the density of the solid and microcellular Engage vulcanizates respectively. Fig. 2 shows the variation of cell density

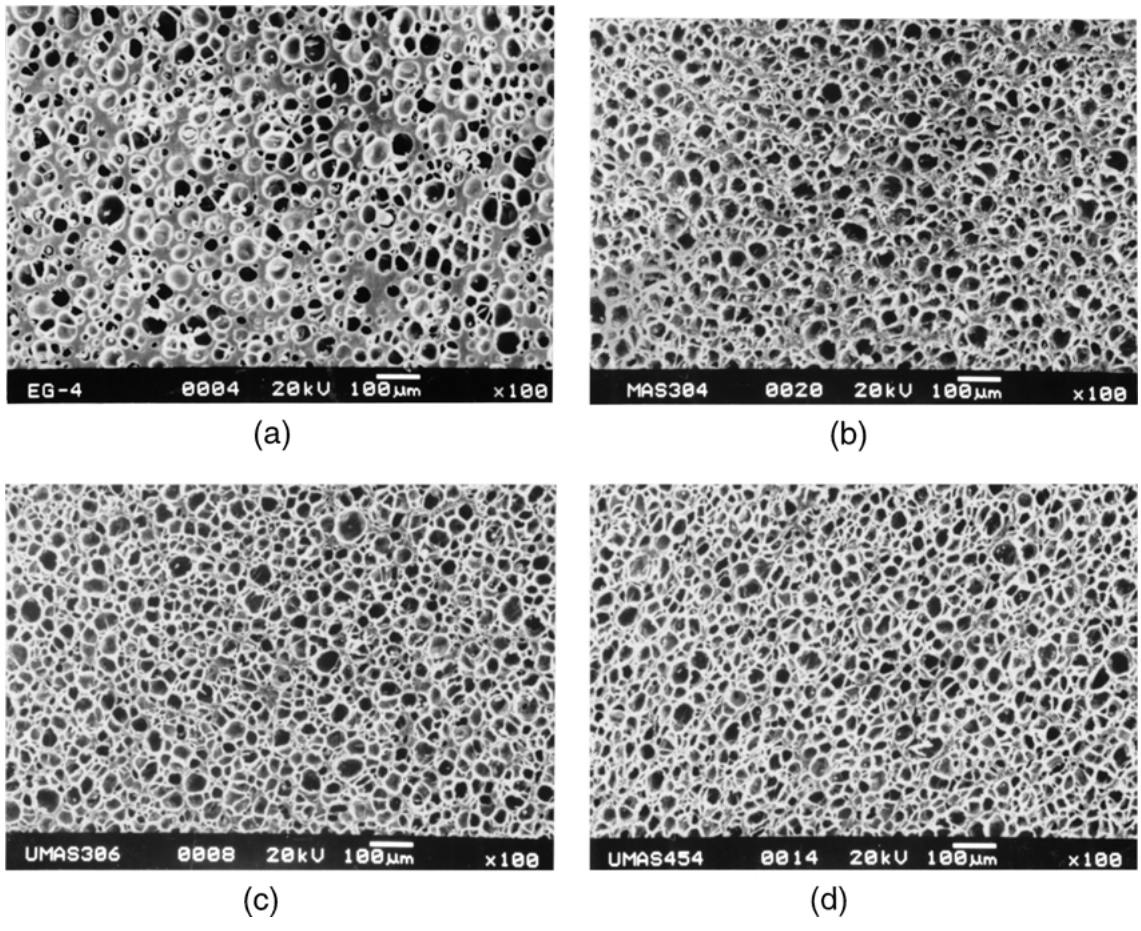

Figure 1 SEM photomicrograph of razor cut surfaces of microcellular Engage vulcanizates: (a) G_4; (b) EAS_3; (c) EAS_4; (d) EAS_7.

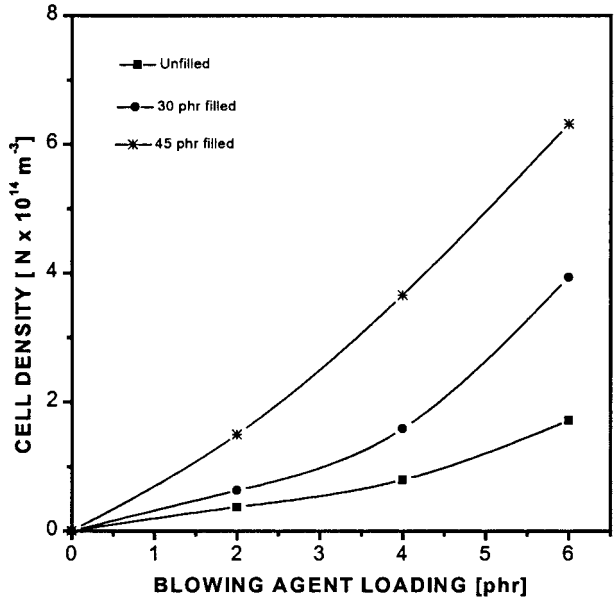

Figure 2 Cell density (N) of microcellular Engage vulcanizates: effect of blowing agent and filler loading.

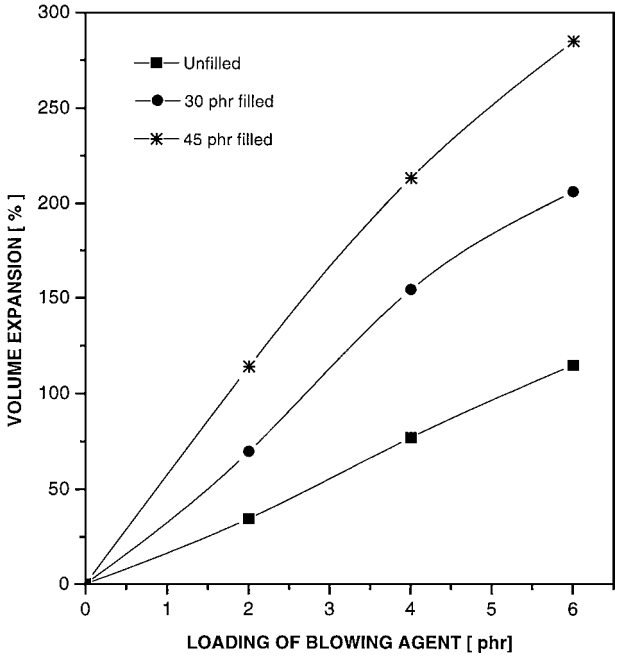

Figure 3 Variation of volume expansion (%) with blowing agent loading.

with blowing agent loading for both unfilled as well as filled vulcanizates. It is seen that cell density increases with increasing blowing agent loading. With incorporation of filler, the cell density is further enhanced as has been explained above.

3.3. Physical properties

Percent of volume expansion of the Engage vulcanizates are shown in Fig. 3. It is observed that % of volume expansion increases with increase in loading of both blowing agent and aluminium silicate filler. Increase in % volume expansion is due to more decomposition of blowing agent and less diffusion

TABLE IV Physical properties of unfilled and aluminium silicate filled microcellular vulcanizates

Mix no.	Tensile strength (Mpa)	Elongation at break (%)	Modulus (100%) (Mpa)	Modulus (200%) (Mpa)	Modulus (300%) (Mpa)	Tear strength (N/mm)
G_0	18.1	1157.7	2.23	2.96	3.6	35
G_2	4.2	573.2	1.51	2.13	2.7	24.5
G_4	3.4	501.3	1.12	1.72	2.31	19.38
G_6	2.7	406	0.94	1.5	2.10	13.6
EAS_1	11.6	912.13	2.86	3.22	3.63	38.96
EAS_2	5.9	656	1.78	2.35	2.94	22.51
EAS_3	4.1	544	1.24	1.82	2.41	15.72
EAS_4	3.3	507	0.86	1.38	1.95	11.32
EAS_5	10.94	893	3.22	3.48	3.81	40.43
EAS_6	5	618	1.68	2.2	2.69	23.43
EAS_7	2.5	435	1.02	1.52	1.98	14.79
EAS_8	2.2	351	0.85	1.52	1.82	10.62

of decomposed gas during curing. Physical properties like relative density, hardness are given in Table III. The relative density decreases with increasing blowing agent loading for both unfilled and filled vulcanizates. The hardness of of the closed–cell unfilled and filled microcellular POE decreases with increasing blowing agent loading. As the enclosed gas in the closed cell has little elastic property, hardness decreases with decreasing relative density. Tensile strength, elongation at break, modulus and tear strength values are given in Table IV. Tensile strength, elongation at break and modulus values decreases with increasing blowing agent loading. In case of solid vulcanizates, tensile strength and elongation at break decreases with increasing concentration of filler loading where as modulus increases marginally. This can be attributed to the fact that due to high polar surface of silicate filler, polymer-filler interaction is weak. Moreover these rigid fillers can act as defects and stress raiser in the composites when the interfacial adhesion between filler and matrix is not strong [28] which is the case with Engage and silicate filler. Tear strength also decreases with increasing blowing agent loading in case of both unfilled as well as silicate filled microcellular vulcanizates. It is observed from the Fig. 4a and b that tensile strength, tear energy, modulus (100%) and hardness varies linearly with foam densities. The tear energy, which is the amount of work required to advance a tear by unit distance in a specimen of unit thickness, is a function of the average diameter of the pores and their distribution [13]. Fig. 5 shows the relative modulus (σ_m/σ_s) and relative tensile strength (E_m/E_s) of 45 phr aluminium silicate loaded closed cell microcellular vulcanizates plotted against relative density (ρ_m/ρ_s). The relative modulus, 100, 200, and 300%, and relative tensile strength decreases linearly with decrease in the relative density. Similar trend is also obtained with 30 phr filler loading. The decrease in relative tensile strength is more sharper than the decrease in relative modulus. The maximum flaw size i.e., flaws, affect the tensile strength but not the modulus. Therefore relative tensile strength behave differently than the relative modulus. It is also observed that the 300% relative modulus shows higher value than 100 and 200% relative modulus. According to additive rule, if

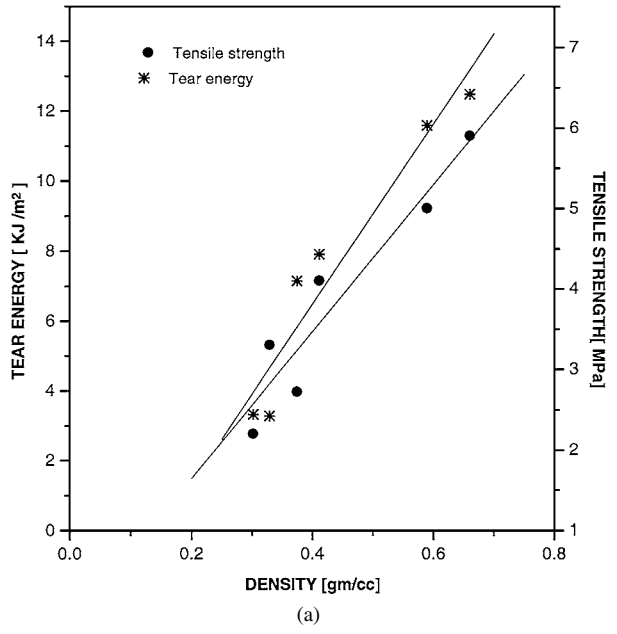

(a)

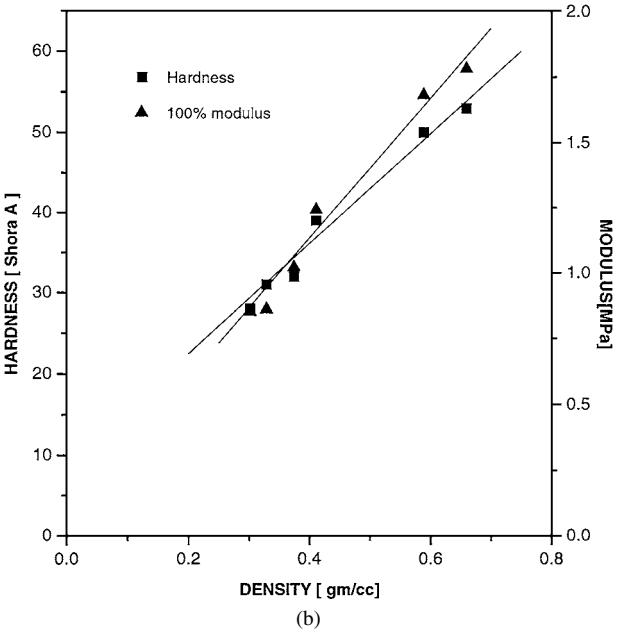

(b)

Figure 4 (a) Variation of tensile strength and tear energy with density of microcellular vulcanizates. (b) Variation of hardness and modulus (100%) with density of microcellular vulcanizates.

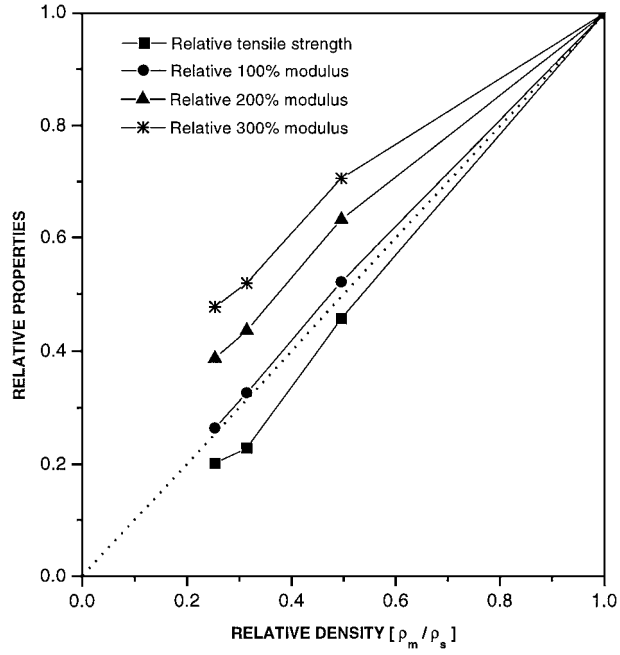

Figure 5 Effect of relative density (ρ_f/ρ_s) on relative properties of 45 phr aluminium silicate filled microcellular vulcanizate.

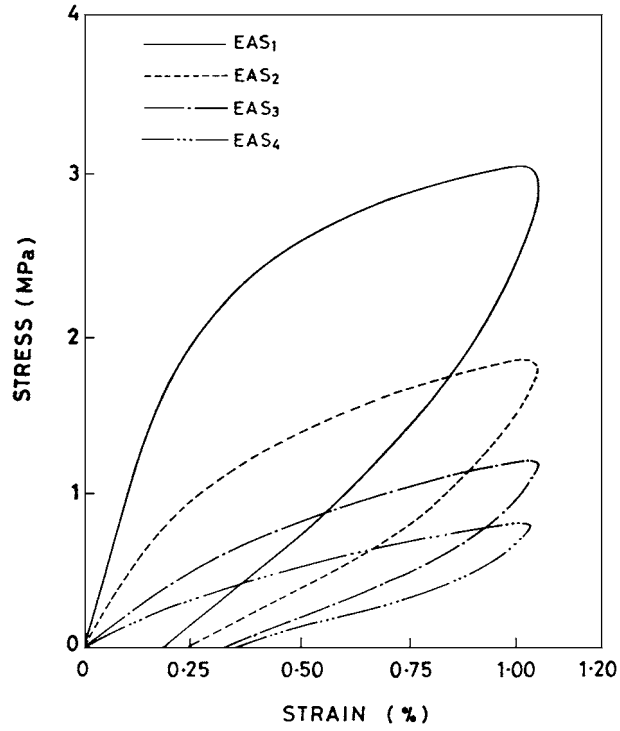

Figure 6 Hysteresis curves of 30 phr aluminium silicate filled vulcanizates.

the modulus depends only on relative density than it will follow the line joining (0, 0) and (1, 1) points. So this increase in relative modulus may be due to the increase in enclosed gas pressure inside the cells [26].

Fig. 6 shows the hysteresis loss of 30 phr aluminium silicate filled solid and microcellular vulcanizates at 100% elongation. Table V summarizes the hysteresis loss values of different vulcanizates at 100% elongation. The hysteresis loss values of microcellular vulcanizates are found to decrease with increase in blowing agent concentration. This is true for all cycles of measurement and for all filler loading. Where as with incorporation of aluminium silicate filler, vulcanizates exhibit increased hysteresis loss with incorporation of silicate filler. This phenomenon may be attributed to the filler-rubber slippage mechanism [29]. The solid vulcanizates have higher hysteresis loss than their corresponding microcellular vulcanizates. The lower hysteresis loss values of microcellular Engage vulcanizates as compared to the solid vulcanizates and the decrease in hysteresis loss with increase in blowing agent concentration can be attributed to the low energy absorption values of closed cells. The % set of the microcellular vulcanizates after 3rd cycle in the hysteresis test were found to be lower compared to the solid vulcanizates. These values decreases with increasing blowing agent loading at a given filler loading and increased with the incorporation of silicate filler at a particular blowing agent concentration. This phenomenon can be attributed to the highly resilient nature of the closed cell microcellular vulcanizates.

TABLE V Result of hysteresis studies of unfilled and aluminium silicate filled microcellular engage vulcanizates

Mix no.	Hysteresis loss in J/m^2 at 100% Elongation. 1st Cycle	2nd Cycle	3rd Cycle	% Set after 3rd Cycle
G_0	0.035	0.022	0.018	6.6
G_2	0.028	0.015	0.013	5.6
G_4	0.021	0.011	0.010	4.4
G_6	0.018	0.009	0.008	3.4
EAS_1	0.063	0.027	0.022	13.3
EAS_2	0.034	0.015	0.013	10
EAS_3	0.021	0.010	0.009	8.3
EAS_4	0.014	0.006	0.006	5
EAS_5	0.073	0.027	0.023	21.6
EAS_6	0.033	0.014	0.012	11.66
EAS_7	0.019	0.008	0.007	8.3
EAS_8	0.012	0.005	0.005	5

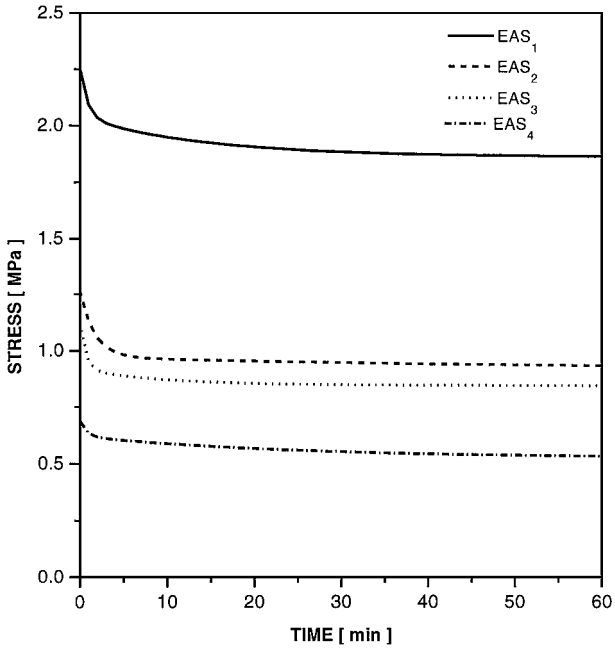

Figure 7 Stress relaxation behavior of 30 phr aluminium silicate filled closed-cell microcellular vulcanizates.

The stress relaxation behavior of closed cell microcellular vulcanizates is determined by stretching the samples at a constant strain level of 100%. Figs 7 and 8 show the decay of stress with time for 30 and 45 phr silicate filled vulcanizates respectively. Initially the rate of decay is more prominent in case of 45 phr silicate filled solid vulcanizates than that of 30 phr solid vulcanizates which may be attributed to poor polymer-filler interaction. The nature of decay is almost similar to closed cell microcellular vulcanizates. Thus the relaxation behaviour is independent of blowing agent [26, 27].

3.4. Fracture nuclei in tensile failure

The tearing energy of the foam, T_f, can be expressed as [11]

$$T_f = 2KE_f l \tag{2}$$

where K, is a numerical constant having a value of about 2. l is the depth of the flaw, and E_f is the strain energy density at failure in the bulk of the test piece for the foam. According to tearing energy criterion developed by Rivlin and Thomas [30], it can be assumed that tensile rupture occurs by catastrophic tearing of the flaw and is described by Equation 2. In the present work, the flaw depths of the microcellular Engage vulcanizates were calculated from Equation 2 using the measured tear energy and strain energy density of the microcellular vulcanizates. The tear energy was calculated from the tear strength using the trouser specimen (ASTM D-3574). The following equation was used for calculation of tear strength:

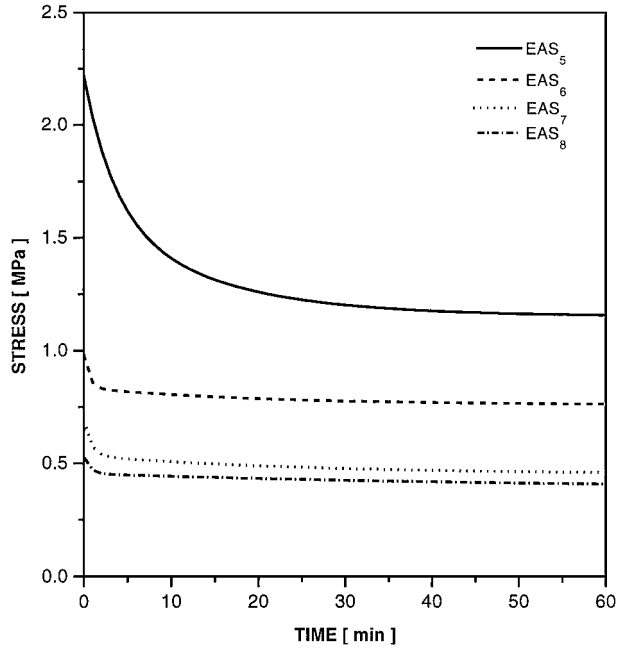

Figure 8 Stress relaxation behavior of 45 phr aluminium silicate filled closed-cell microcellular vulcanizates.

$$T_f = 2 \times F/t$$

$$T_f = 2 \times T_f' \tag{3}$$

where T_f' is the trouser tear strength and T_f is the tear energy. Strain energy density can be calculated from the tensile strength and the elongation at break of the dumbbell-shaped specimen. The results are summarized in Table VI. It is observed that theoretical values of the flaws depth (l) are larger than the corresponding maximum cell size. The mean value of the ratio of the

TABLE VI Tear energy and calculated flaw size of unfilled and aluminium silicate filled microcellular engage vulcanizates

Mix no.	Trouser tear resistance (N/mm)	Tear Energy (T_f) (KJ/m^2)	Strain energy density (KJ/m^2)	Calculated cell size (I) (μm)
G_2	4.79	9.58	12033	199
G_4	3.56	7.12	8517	208
G_6	1.77	3.54	5479	161
EAS_2	12.5	12.5	19352	161
EAS_3	7.91	7.91	11152	177
EAS_4	3.28	3.28	8365.5	98
EAS_6	11.16	11.16	15454	180.5
EAS_7	7.15	7.15	10794	165
EAS_8	3.32	3.32	5425	153

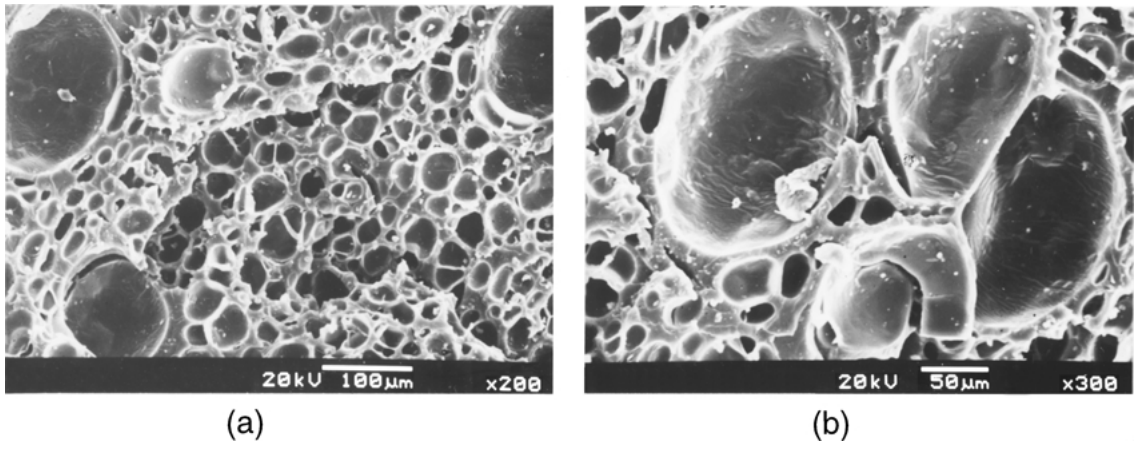

Figure 9 SEM photomicrograph of tensile fracture surfaces of (a) EAS_2 (b) EAS_6.

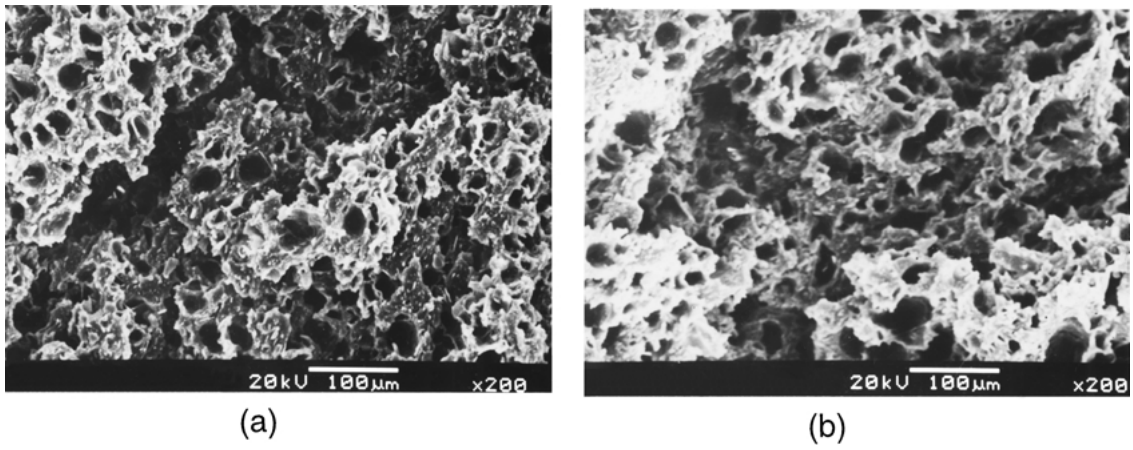

Figure 10 SEM photomicrograph of tear fracture surfaces of (a) EAS_2 (b) EAS_6.

theoretical depth of the flaws and the maximum cell size is about 2.57. According to Gent and Thomas [11], for a perfectly regular foam structure, the tear tip diameter would be expected to be twice the pore diameter due to random arrangement of pores in space. Imperfections in the foam will lead to local deviations of tear from a linear front and hence give rise to a corresponding larger effective diameter at the tip.

3.5. Tensile fracture

Fig. 9a and b demonstrates SEM photomicrographs of tensile fracture surfaces of 2 phr blowing agent loaded 30 and 45 phr aluminium silicate filled microcellular respectevily. In case of Fig. 9a it can be seen that there is collapse of bigger cells with formation of vacuoles and Fig. 9b shows the propagation of the tensile rupture paths from the bigger cells. This can be attributed to the inability of the inorganic fillers for reinforcement i.,e. weak bonding and low interaction with the hydrocarbon rubber phase, difficult dispersion of the silicates and cure retardation and low states of cure due to acidic surface characteristics. At high strain, rupture is initiated by the formation of vacuoles at the filler rubber interface [31].

3.6. Tear fracture

Fig. 10a and b shows the SEM fractograph of tear fracture surfaces of 2 phr blowing agent loaded 30 and 45 phr aluminium silicate filled microcellular vulcanizate respectively. In all the cases it can be observed that the failure is catastrophic in nature which leads to de-lamination. When tensile force is applied to the material, it is considered to be uniform through out the tensile specimen, but concentration of stress builds up at the bigger cells. Failure starts at those points where the actual stress applied is much higher than the bulk of the specimen. Once the failure starts, it proceeds as catastrophic tear giving rise to layer surface with number of tear lines [32]. In these cases the layer delamination is prominent. When tensile force is applied to the material, it is also concentrated in the vicinity of the interfaces of filler particle and polymer matrix. In this region, the stress level is considerably higher than the average value [33]. Weak filler-polymer interaction also leads to formation of loose agglomerates in the matrix which acts as stress raiser [34] and provides easy path for catastrophic failure.

4. Conclusions

1. In case of microcellular Engage vulcanizates, the maximum rheometric torque decreases with increase in blowing agent loading.

2. Average cell size decreases from 27 μm to 25 μm in 30 phr and from 26 μm to 24 μm in 45 phr aluminium silicate filled vulcanizates with incorporation of 2 to 6 phr blowing agent.

3. Cell density and % volume expansion increases with increasing blowing agent loading as well as aluminium silicate filler loading. Thus silicate filler acts as nucleating agent.

4. Tensile strength, modulus (100%), tear energy and hardness varies linearly with the density of the microcellular vulcanizates.

5. Relative density decreases with increasing concentration of blowing agent.

6. Physical properties like tensile strength. elongation at break, modulus decreases with increasing concentration of blowing agent.

7. Enclosed gas pressure in the closed cell increase the relative modulus in aluminium silicate filled vulcanizate where as relative tensile strength decreases sharply which does not obey additive rule.

8. The stress relaxation behavior is independent of blowing agent loading.

9. The hysteresis loss decreases with increasing blowing agent as well as filler loading.

10. Set properties are found to improve with increasing blowing agent concentration.

11. It is observed that theoretically calculated flaw sizes in tensile rupture is about 2.57 times larger than the maximum cell size measured from SEM photomicrographs which suggests that tear path deviates from the linear front and give rise to larger effective depth of the flaws.

12. SEM fractograph studies of tensile and tear fracture surfaces of microcellular vulcanizate reveal that the mechanism of fracture is dependent on the concentration of blowing agent and aluminium silicate filler.

References

1. M. A. RODRIGUEZ PEREZ, J. I. VELASCO, D. ARENCON, O. ALMANZA and J. A. DE SAJA, *J. Appl. Polym. Sci*. **75** (2000) 156.
2. S. C. SMITH, *Kautsch Gummi Kunstst* **51** (1998) 504.
3. S. BENSON, J. MINIK, A. MOET, S. CHUM, A. HILTNER and E. BAER, *J. Polym. Sci: Part B: Polymer Physics*. **34** (1996) 1301.
4. M. W. AARTS and L. FANICHET, *Kautsch Gummi Kunstst* **48** (1995) 497.
5. C. U. BHATT, J. R. ROYER, C. R. HWANG and S. A. KHAN, *J. Polym. Sci: Part B: Polymer Physics* **37** (1999) 1045.
6. C. S. WANG, *J. Appl. Polym. Sci*. **27** (1982) 1205.
7. J. H. AUBERT, *J. Cell Plast*. **24** (1988) 132.
8. L. J. GIBSON and M. F. ASHBY, in "Cellular Solids, Structure and Properties" (Pergamon Press, Oxford, 1988).
9. R. W. PAKALA, C. T. ALVISCO and J. D. LEMAY, *J. Non-Crystal Solids* **125** (1990) 67.
10. L. J. GIBSON, *Mater. Sci. Eng.* A **110** (1984) 1.
11. A. N. GENT and A. G. THOMAS, *J. Appl. Polym. Sci*. **2** (1959) 354.
12. *Idem*., *ibid*. **1** (1959) 107.
13. *Idem*., *Rubb. Chem. Technol*. **36** (1963) 597.
14. J. M. LEDERMAN, *J. Appl. Polym. Sci*. **15** (1971) 693.
15. C. W. STEWART, *J. Polym. Sci*. **A 2** (1970) 8.
16. J. H. EXELBY, *Plast. Rubb. Comp. Proc. Appl*. **15** (1991) 213.
17. A. DUTTA and M. CAKMAK, *Rubb. Chem. Technol*. **65** (1992) 778.
18. N. SRAMESH, D. H. RASMUSSEN and G. A. CAMBELL, *Polym. Eng. Sci*. **31**(23) (1991) 1657.
19. J. S. COTTON and N. P. SUH, *Polym. Eng. Sci*. **27** (1987) 493.
20. V. KUMAR and N. P. SUH, *ibid*. **30** (1990) 1323.
21. R. E. WHITTEKER, *J. Appl. Polym. Sci*. **15** (1971) 1205.
22. P. D. AGARWAL and K. E. KEAR, *Rubber World* **201** (1990) 20.
23. C. HEPBURN and N. ALAM, *Cell Polym*. **10** (1991) 99.
24. K. MUKHOPADHYAY, D. K. TRIPATHY and S. K. DE, *Rubb. Chem. Technol*. **66** (1993) 38.
25. K. C. GURYA and D. K. TRIPATHY, *Plast. Rubb. Comp. Proc. Appl*. **23** (1995) 195.
26. *Idem*., *J. Appl. Polym. Sci*. **62** (1996) 117.
27. N. C. NAYAK and D. K. TRIPATHY, *Cell Polym*. **19** (2000) 271.
28. Z. DEMJEN, B. PUKANSKY and J. NAGY, *Composites* **29A** (1998) 323.
29. J. A. C. HARWOOD, L. MULLIN and A. R. PYNE, *J. Appl. Polym. Sci*. **9** (1965) 3011.
30. R. S. RIVLIN and A. G. THOMAS, *J. Polym. Sci*. **10** (1953) 291.
31. E. M. DANNENBERG, *Rubb. Chem. Tecgnol*. **55** (1982) 866.
32. S. K. CHAKRAVARTY and S. K. DE, *Polymer.* **24** (1983) 1061.
33. G. WYPYCH, Fillers (ChemTec Publishing, Ontario, Canada, 1993) p. 203–205.
34. N. M. MATHEW and S. K. DE, *Polymer.* **23** (1982) 632.

Received 14 February
and accepted 2 November 2001